Low temperature SiN waveguides optimization for photonic platform

Eva Kempf[3,1], M. Calvo[3,1], Florian Domengie[3], Stéphane Monfray[3], Frederic Boeuf[3], Paul Charette[2], Régis Orobtchouk[1]

[1]*Institut des Nanotechnologies de Lyon (INL), CNRS UMR5270, INSA de Lyon, 7 avenue Jean Capelle 69621 Villeurbanne Cedex – France*

[2]Laboratoire Nanotechnologies Nanosystèmes (LN2)-CNRS UMI-3463, Université de Sherbrooke, Sherbrooke, Québec, J1K 0A5, Canada

[3]STMicroelectronics, 850 Rue Jean Monnet, Crolles, 38920, France

ABSTRACT

Integration of SiN on Si photonics platform becomes attractive for 3D integration of different waveguide levels in an optical routing circuit, and can be used for the realization of athermal devices needing specifics group index or group velocity dispersion. This paper is focused on the determination of the optical properties of different SiN deposited by PVD (Plasma Vapor Deposition) and PECVD (Plasma Enhanced Plasma Vapor Deposition) equipment with temperatures lower than 400°C to keep the compatibility with CMOS process. A set of designs including optical routing basic building blocks such as bends, MMI splitters and asymmetric Mach-Zehnder interferometer has been designed to determine propagation losses and propagation constants with high accuracy, for a large spectral range, around 1.31µm and 1.55µm [1].

Devices were manufactured on the STMicroelectronics DAPHNE (Datacom Advanced Photonics Nanoscale Environment) 300 mm Photonic R&D platform [2]. Comparison of experimental data with theoretical models will be made. Especially, we discuss the development of Finite Difference Full Vectorial mode solvers [3-4] coupled with the Mode Matching method. This method, used to simulate the propagation of light, also allows to evaluate side wall roughness contributions, Rayleigh scattering and absorption due to 2nd harmonic vibrations of Si-OH and N-H bonds.

Keywords: Si photonics, SiN waveguide, MMI splitter, asymmetric Mach Zehnder interferometer

1. INTRODUCTION

Development of SiN platforms have been the subject of a large development this last decade to overcome some limitation of silicon such as lower thermal conductivity, band gap exceeding 4 eV and a lower refractive index contrast allowing the possibility of realization of athermal devices, avoiding two photon absorption for the transmission of high power and reduction of propagation losses. Different multilayer Silicon Nitride-on-Silicon Photonic Integrated Platform are now available in the world using LPCVD and PECVD deposition processes. Low-Pressure Chemical Vapour Deposition (LPCVD) at high temperature (>700°C) is required to avoid the N-H and Si-H bonds absorption existing in the C-band. Ligentec's thick SiN platform has been used for the realization of an optical-frequency synthetizer [5] and a photonic chip based on optical frequency comb [6]. Low loss optical waveguide [7] and basic building blocks for optical routing [8-9] are developed on the LioniX International TriPleX platform and optical sensors with the AMO's Silicon Nitride Photonic Platform: Full Custom Pilot Line Services [10-12]. More fully CMOS compatible Plasma Enhanced Chemical Vapour Deposition (PECVD) at low temperature (<400 °C) are also available at the BioPIX SiN platform of IMEC [9].

This paper presents design and optical characterization of basic building blocks for optical routing made with the 300mm PECVD/PVD DAPHNE SiN platform of STMicroelectronics.

2. SiN deposition process

The PECVD SiN deposition is carried out at a temperature above 400°C. One drawback of the vapour-phase deposition is the creation of –NH bonds which absorb light around 1550nm, a widely used wavelength in the field of telecommunications. Therefore, PVD depositions with different concentrations of silicon were made in order to attempt to decrease absorption loss. The PVD deposition at 200°C was carried out by the sputtering of a Si target. A radiofrequency (RF) plasma of Argon and Nitrogen with a variable stoechimoetry was used in order to control the optical index of the deposited material.

	n(1.31µm)	n(1.55µm)	SiN thickness
PVD	1.944	1.942	632 ± 8 nm
Si-rich PVD	1.989	1.985	627 ± 16 nm
PECVD	1.913	1.910	600 ± 20 nm

Table 2.1. Thickness of the deposited SiN films and computed optical indexes.

These depositions were made on 300mm wafers with a silicon substrate and a 2µm layer of thermal SiO_2. Waveguides were patterned using DeepUV lithography and Reactive Ion Etching (RIE) process, and were encapsulated in TEOS SiO_2.

The table 2.1 gives the thickness of the fabricated SiN films as well as their optical index. The values of the optical indexes were computed applying Cauchy dispersion laws to ellipsometry measurements.

3 Buiding blocks.

Modelings are performed with Full Vectorial Finite Difference mode solvers in Cartesian and cylindrical coordinates respectively for the design of straight and bend waveguide [3-4]. Transparent boundary conditions are added for the calculation of propagation losses induces by the leakage through the buried silica layer and the radiation effect inherent to the bend. A waveguide width of about 700 nm is chosen to preserve a single mode condition for a spectral range between 1.2 and 1.7 µm and for all the materials involve in this study. A 2 µm thick buried silica layer and 40 µm bend radius are enough to obtain bending losses lower than 0.1 dB. Effective indexes of the TE like mode are given in the table 1:

	1310nm	1550nm
PECVD	1.6492	1.5861
PVD	1.6831	1.6193
Si-rich PVD	1.7200	1.6500

Table 1. Effective indexes of the 700nm wide waveguides at 1310nm and 1550nm.

Mode matching method (MMM) is used to calculate propagation losses induced by the sidewall roughness. Firstly, two independant random surfaces with Gaussian statistic (σ = 2 nm and L_c = 50 nm) are generated and added on both lateral sides of the waveguide. Segmented approach is then applied to calculate a set of guided and radiative modes in all of the local waveguides generated. Mode Matching algorithm gives propagation losses thanks to the reduction of power transmission after the propagation in a 20 µm long waveguide with a discretization of 1 nm (corresponding to 20 000 local waveguides). We can notice that losses of 1 dB/cm require an accuracy on the transmission coefficient of about 10^{-7}, the accuracy on the orthogonality relations between the different modes. It can be evaluated with the mode solvers of commercial softwares, which are calculating an averaging of the refractive indexes at each boundaries to overcome instabilities due to the discontinuity of the normal components of the electrical field. This limitation is overcome with a nine points stencil discretization scheme [3] giving an accuracy of 10^{-17}. The propagation losses induced by the sidewall roughness are respectively of 0.04 and 0.16 dB/cm at λ = 1.31 and 1.55 µm.

Design of MMI splitter is also performed with MMM. As the broadening of the spectral bandwidth increases with the reduction of the MMI footprint, the minimum width of 3.2 µm is require to have 5 different guided modes in both polarizations providing good images of the input waveguide at the output and a reduction of scattering losses lower than 0.1 dB (see fig.1), resulting on a 7.7 µm long splitter.

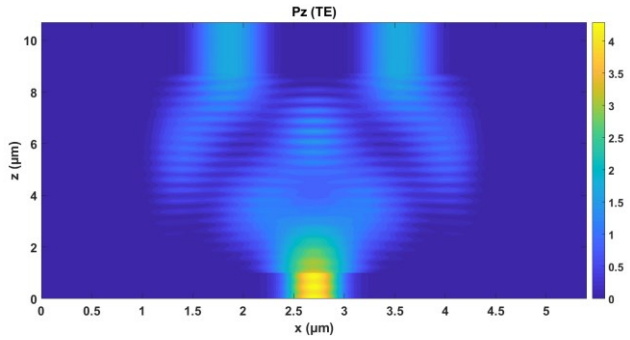

Fig 1 : Mapping of light power in the SiN MMI splitter (W_{MMI} = 3.2 µm, L_{MMI} = 7.7 µm).

All of the basic building blocks are merged to design a set of optical test devices for an accurate characterization of propagation losses and dispersion curves of the SiN waveguides.

4 Optical test devices

The characterization of the deposited SiN was carried out for the TE mode both around 1310 and 1550nm where the NH and OH absorption pics are located. Light injection was performed with butt coupling and polarization maintaining fibers, and the data were collected using an Optical Spectrum Analyzer (OSA). Different structures, presented in fig. 2, were fabricated.

In order to determine optical propagation losses, the light was injected into three spirals of respective length 4.2cm, 7cm and 9.8cm with 142 bends of constant radius 40µm. The waveguides width is equal to 700nm ± 6nm. For each wavelength, a linear regression was done using the optical power detected at the end of each

spiral and error bars were computed with the standard error of the linear regression. This set up was then improved by using three waveguides of respective length 1mm, 2mm and 3mm, with 3 bends of constant radius and, for each waveguide, a reference arm. The measurement arm and the reference arm are separated by a 1x2 Multi-mode interferometer (MMI), allowing a more accurate measurement.

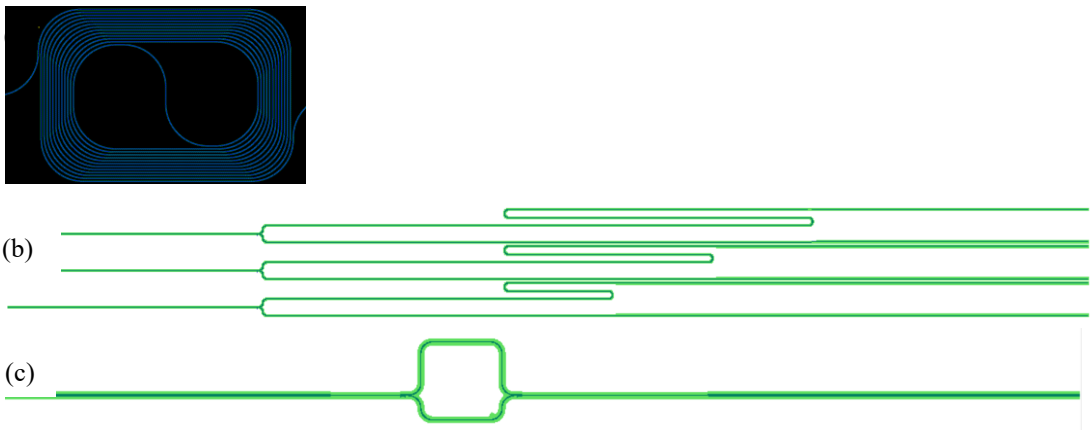

Figure 2. Fabricated structures for optical characterization : (a) Spirals, (b) Waveguides with 1x2 MMI, measurement and reference arms, (c) Asymmetric Mach-Zehnder interferometer.

An asymmetric Mach-Zehnder interferometer (MZI) was also designed in order to extract the effective index dependance with the wavelength. Identical structures with different waveguide width, respectively 500nm ± 6nm and 600nm ± 6nm were fabricated. The input light is split into two with a 1x2 MMI, it propagates into the two arms of different length and is recombined at the end of the dispositive with a 2x1 MMI. The optical power at the end of the interferometer can be expressed as :

$$P=P_{max}.\cos^2\left(\frac{\pi.n_{eff}.\Delta L}{\lambda}\right) \quad (1)$$

Where P_{max} is the optical power at the input of the interferometer, n_{eff} is the optical effective index of the waveguide, ΔL is the difference of length between the two arms of the interferometer ΔL =100µm, and λ is the optical wavelength. The output power at the end of the interferometer can be modelled as a function of the wavelength as:

$$n_{eff}(\lambda_m)=a_1+a_2\lambda_m+a_3\lambda_m^2 \quad (2)$$

where a_1, a_2 and a_3 are coefficients that can be experimentally obtained with non-linear regression routine.

5 Experimental results

Figure 3 shows the propagation losses of the three different characterized SiN films. While the film grow by PECVD presents low losses at 1310nm (- 0.81 ± 0.23 dB/cm), the –NH absorption peak causes the losses to drop at 1550nm (- 2.42 ± 0.97 dB/cm).

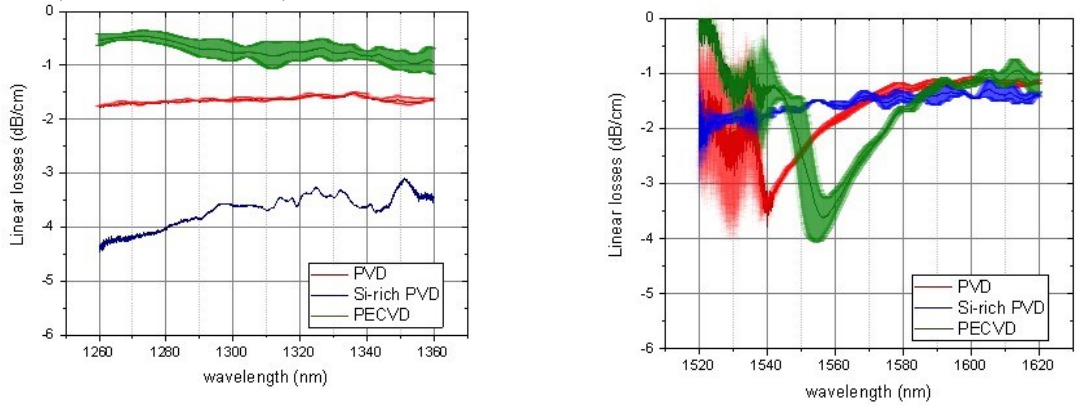

Figure 3:Propagation losses measurement for the 2 kind of SiN materials in the spectral range around 1.31 and 1.55 µm.

On the contrary, the Si-rich PVD film displays losses as high as -3.68 dB/cm at 1310nm. As the signal was so weak at the output of the longest spiral, only the two shortest spirals could be used for this measurement. However, at 1550nm, the losses are much weaker as for the PECVD film, with only 1.68 ± 0.023 dB/cm.

The parameters $\boldsymbol{a_1}$, $\boldsymbol{a_2}$, $\boldsymbol{a_3}$ computed by our 2nd order polynomial model as well as experimentally measured, are given in the table 2. These results show that the experimental values fit in very well with the theoretical ones.

	a_1	$\boldsymbol{a_2}$	a_3	ΔL
PVD 600nm th.	2.034062	-0.207522	-0.128849	
PVD 600nm exp.	2.031722	-0.207645	-0.137300	98.54
Si-rich PVD 600nm th.	1.863318	0.255719	-0.461235	
Si-rich PVD 600nm exp.	1.863764	0.274002	-0.445412	
PVD 500nm th.	2.077636	-0.327296	-0.069350	
PVD 500nm exp.	2.077583	-0.336101	-0.069309	98.40
Si-rich PVD 500nm th.	2.150775	-0.349366	-0.084709	
Si-rich PVD 500nm exp.	2.150789	-0.348823	-0.085166	99.58

Table 2. Theoretical and experimental values of the coefficients of the 2nd order polynomial modelling the effective index as a function of the wavelength.

6 CONCLUSION

A SiN PVD film with an optical index of 1.99 shows reduced propagation losses comparing to the usual PECVD SiN fabricated by STMicroelectronics. Losses as low as 1.68 dB/cm were measured at 1550nm. This value could be even decreased by increasing the film density. The other advantages of this method is the lower temperature required for the process, 200°C, which is compatible with the CMOS process and the suppression of losses induce by N-H and O-H bonds absorption.

This study has also allowed validating our model of 2nd order polynomial dependence of the optical effective index with wavelength using asymmetrical Mach-Zehnder interferometers. A good precision up to the third decimal of the coefficients was obtained.

ACKNOWLEDGEMENTS

This work is supported by a European IPCEI program.

REFERENCES

[1] G. Fan et al., "Optical waveguides on three material platforms of silicon-on insulator, amorphous silicon and silicon nitride," IEEE J. Sel. Top. Quantum Electron. 22, 225 (2016).

[2] S. Guerber et al., "Integrated SiN on SOI dual photonic devices for advanced datacom solutions," Silicon Photonics: From Fundamental Research to Manufacturing (Strasbourg, France), p. 3, (2018).

[3] X. Hu et al., "Modeling the anisotropic electro-optic interaction in hybrid silicon-ferroelectric optical modulator," Opt. Express 23, 1699 (2015).

[4] M. Masi et all., "Towards a realistic modelling of ultra-compact racetrack resonators," J. Lightwave Technol. 28, 3233 (2010).

[5] D. T. Spencer et al., An optical-frequency synthesizer using integrated photonics, Nature, volume 557, pages8185 (2018).

[6] Brasch et al., Photonic chip based optical frequency comb using soliton Cherenkow radiation, Vol. 351, Issue 6271, pp. 357-360 Science (2016).

[7] C. G. Roeloffzen et al., Low-loss Si3N4 TriPleX optical waveguides: Technology and applications overview, IEEE journal of selected topics in quantum electronics, vol. 24, no. 4, pp. 121, 2018.

[8] K. Worhoff et al., TriPleX: a versatile dielectric photonic platform, Advanced Optical Technologies, vol. 4, no. 2, pp. 189207, 2015.

[9] PiX4life Pilot line. www.pix4life.eu.

[10] P. Munoz et al., Silicon nitride photonic integration platforms for visible, near-infrared and mid-infrared applications, Sensors 17(9), 2088 (2017).

[11] K. E. Zinoviev et al., Integrated Bimodal Waveguide Interferometric Biosensor for Label-Free Analysis, J. Light. Technol. 29 (13), 1926 (2011).

[12] J.-C. Tinguely, Ø. I. Helle, and B. S. Ahluwalia, Silicon Nitride Waveguide Platform for Fluores-cence Microscopy of Living Cells, Opt. Express, 25 (22), 27678 (2017).